JCTC Journal of Chemical Theory and Computation

Letter

pubs.acs.org/JCTC

The $Fe^{III}(H_2O_2)$ Complex as a Highly Efficient Oxidant in Sulfoxidation Reactions: Revival of an Underrated Oxidant in Cytochrome P450

Binju Wang,[†] Chunsen Li,[†] Kyung-Bin Cho,[‡] Wonwoo Nam,*[,‡] and Sason Shaik*[,†]

[†]Institute of Chemistry and the Lise Meitner-Minerva Center for Computational Quantum Chemistry, The Hebrew University of Jerusalem, 91904 Jerusalem, Israel

[‡]Department of Bioinspired Science, Ewha Womans University, Seoul 120-750, Korea

Supporting Information

ABSTRACT: This work demonstrates that the $Fe^{III}(H_2O_2)$ complex, which has been considered as an unlikely oxidant in P450, is actually very efficient in sulfoxidation reactions. Thus, $Fe^{III}(H_2O_2)$ undergoes a low-barrier nucleophilic attack by sulfur on the distal oxygen, *resulting in heterolytic O−O cleavage coupled to proton transfer*. We further show that $Fe^{III}(H_2O_2)$ is an efficient sulfoxidation catalyst in synthetic iron porphyrin and iron corrolazine compounds. In all cases, $Fe^{III}(H_2O_2)$ performs the oxidation *much faster than it converts to Cpd I* and will therefore bypass Cpd I in the presence of a thioether. Thus, this paper not only suggests a plausible resolution of a longstanding issue in P450 chemistry regarding the "second oxidant" but also highlights a new mechanistic pathway for sulfoxidation reactions in P450s and their multitude of synthetic analogues. These findings have far-reaching implications for transition metal compounds, where H_2O_2 is used as the terminal oxidant.

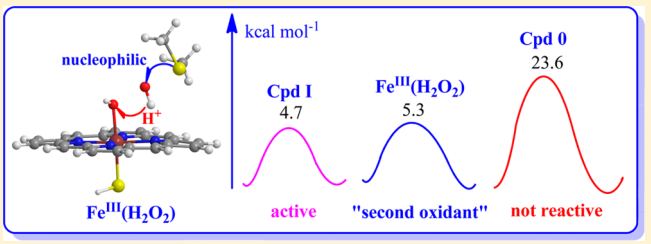

Cytochromes P450 (P450) are versatile enzymes that oxidize a variety of organic substances.[1−6] The current consensus is that the reactive oxidant is the high-valent oxoiron(IV) species, known as compound I (Cpd I). As shown in Scheme 1, the ferrous complex accepts O_2 and then undergoes reduction and two protonation events on the distal oxygen, leading to formation of a water molecule and thereby also Cpd I.

However, if the second protonation occurs on the *proximal* oxygen, this leads to "uncoupling", whereby hydrogen peroxide, H_2O_2, is formed and liberated (see midsection of Scheme 1).[1,3,5,7] Curiously, H_2O_2 and peroxyacids serve at the same time as means of shunting the P450 cycle en route to Cpd I formation.[1−5] In fact, it is a common practice to use H_2O_2 to generate oxoiron(IV) species in heme peroxidase and synthetic nonheme systems.[8−19] However, only seldom[20,21] have H_2O_2 or its ferric complex, by themselves, been considered to be the direct oxidant species. This paper shows a new mechanistic pathway, whereby the $Fe^{III}(H_2O_2)$ complex acts as a highly efficient sulfoxidation catalyst that will bypass Cpd I formation.

Scheme 1. Oxidant Species in P450 Enzymes and Their Interconversion

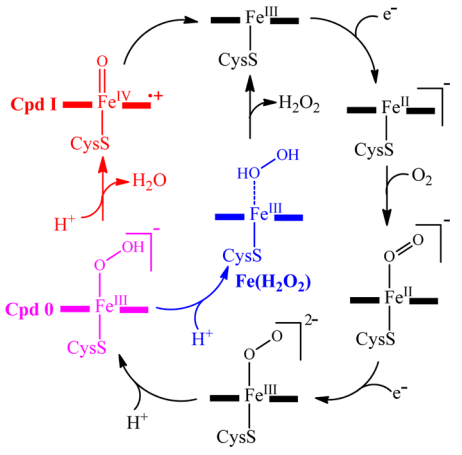

As such, our study revives the longstanding issue in P450 chemistry regarding the potential involvement of an alternative oxidant to Cpd I.[3,5,6,22−31] The indirect evidence for the existence of a second oxidizing species is particularly strong when looking at sulfoxidation reactions of thioether substrates in P450 enzymes[22,23] and its synthetic analogues.[24,25] For instance, the T→A mutation (replacing threonine, T, by alanine, A) in P450 affects the proton delivery that converts Cpd 0 (Scheme 1) to Cpd I.[7,26−29,32−35] This slows down hydroxylation reactions but does not affect sulfoxidation.[23] Similarly, during oxidation of *para*-thiomethoxy-*N*,*N*-dimethylaniline (*p*-CH_3S-DMA) in $P450_{BM3}$, the T268A mutation increased sulfoxidation over N-dealkylation.[22] These results seem to be consistent with sulfoxidation being efficiently mediated by another oxidant so that sulfoxidation appears less affected when the formation of Cpd I is inhibited. A related result is the fact that Fe^{III}-corrolazine uses H_2O_2 to catalyze sulfoxidation, while bypassing the analogous Cpd I species.[24]

Received: March 9, 2013

 © XXXX American Chemical Society dx.doi.org/10.1021/ct400190f | J. Chem. Theory Comput. XXXX, XXX, XXX−XXX

Scheme 2. $Fe^{III}(H_2O_2)$ Complexes, 1−3, and Substrates, S1 (DMS) and S2 (*p*-CH_3S-DMA), Used in This Study

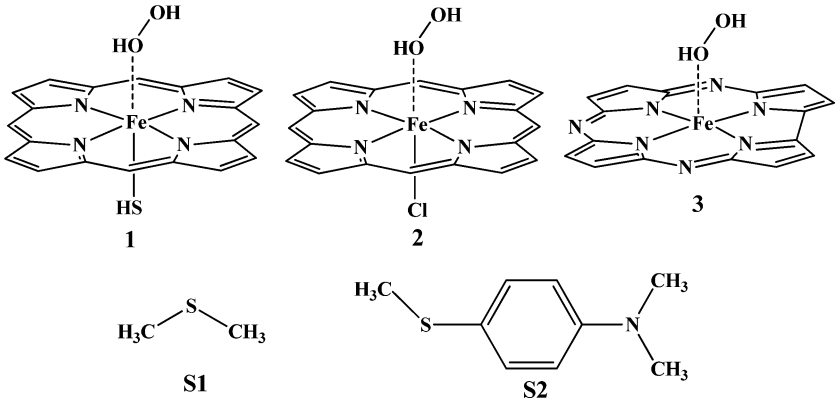

So, all these experimental results support the existence of a potential second oxidant species. But what might this species be?

While initial suggestions of the second P450 oxidant focused on Cpd 0 (Scheme 1), this species was demonstrated to be a sluggish oxidant by both theory[36−38] and experimental results.[39−41] Previous studies of the $Fe^{III}(H_2O_2)$ complex as a potential oxidant focused on an O−O bond homolysis pathway,[38,42] whereby the oxidative activity of $Fe^{III}(H_2O_2)$ was found to be inferior to Cpd I. As shall be demonstrated here by means of density functional calculations, the $Fe^{III}(H_2O_2)$ species in iron−porphyrins and iron−corrolazine complexes can participate in *concerted heterolytic reactions with thioethers and functions as a highly efficient oxidant that bypasses Cpd I*. The generality of this conclusion will be demonstrated below.

To explore the mechanism, we used UB3LYP including solvation corrections (see Methods and the Supporting Information (SI)) to study the three $Fe^{III}(H_2O_2)$ complexes in Scheme 2, **1**−**3** in their reactions with the substrates **S1** (DMS) and **S2** (*p*-CH_3S-DMA). The oxidative capabilities of **1**−**3** were then gauged against those of the corresponding Cpd I and Cpd 0 species.

As shown in Figure 1, the sulfoxidation reactions proceed in a concerted manner, and the corresponding transition state (**TS**) species ^{2}**TS1** involves significant charge separation. Thus, with solvation correction, the doublet state barrier is 5.3 kcal mol^{-1}, while the corresponding gas phase value was 10.5 kcal mol^{-1}, as might be expected from a heterolytic mechanism. To test the effect of the iron−porphine, we calculated the reaction of DMS with bare H_2O_2. The computed barrier of 17.5 kcal mol^{-1} (Figure S3) in the absence of iron−porphine is much larger than the value of 5.3 kcal mol^{-1} calculated in its presence. This is in accord with experiments which have shown that the noncatalyzed reaction is rather slow (the rate constant is about 10^{-2} s^{-1}),[43] and furthermore, the result shows also that the iron porphine acts as a Lewis acid catalyst. Indeed, oxidations by H_2O_2 require generally a catalyst that can promote the heterolytic reaction.[20,21]

The concerted heterolysis mechanism is basically a nucleophilic attack[44] of the sulfur lone pair on the distal oxygen of H_2O_2, wherein the O−O bond cleavage is coupled to proton transfer to form Fe^{III}−OH_2 and $(CH_3)_2SO$ (DMSO). As shown in Figure 2, the IRC reaction path analysis shows that the "concerted" mechanism is asynchronous. It commences as a nucleophilic attack by the S center of DMS on the O_d atom of Fe^{III}−O_p(H)−O_dH. As the heterolytic O_p−O_dH bond cleavage

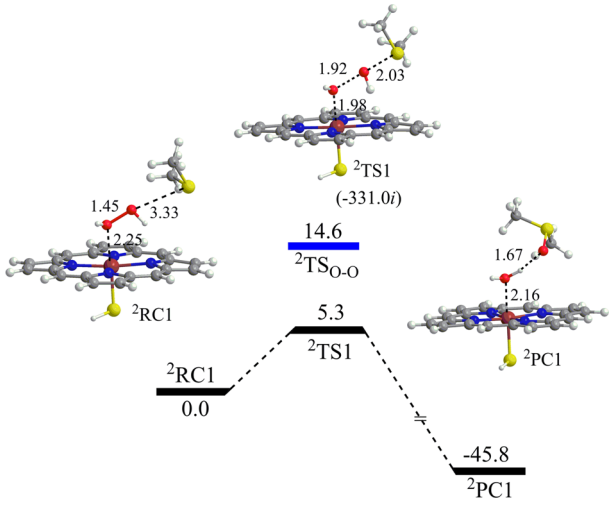

Figure 1. Calculated relative energy profile (in kcal mol^{-1}) and optimized structures (lengths in Å) of species for sulfoxidation of **S1** (DMS) by the $Fe^{III}(H_2O_2)$ complex **1** in the S = 1/2 state. Relative energies are given as E_2 values (UB3LYP/LACV3P++**//LACVP** with solvent correction). The value of the imaginary frequency in cm^{-1} is shown underneath the ^{2}**TS1** structure. The group charge distribution in ^{2}**TS1** is +0.47 on the DMS−OH fragment and −0.47 on the rest (see Table S1). The relative energy of the transition state for the homolysis process (^{2}**TS**$_{O-O}$) is also given by the blue bar for comparison.

in ^{2}**TS1** ensues, en route to the product, the $[HS(Por)Fe^{III}-O_pH]^-$ moiety abstracts the proton from the $HOS(CH_3)_2^+$ moiety, yielding the product complex ^{2}**PC1**. During the entire path, the d-electronic configuration of the iron remains unchanged corresponding to $(\delta_{xy})^2(d_{xz/yz})^3$ and hence to a ferric−porphyrin complex. Since the mechanism involves a nucleophilic attack on the O−O bond, the Fe^{III}−porphyrin complex acts as a Lewis acid that facilitates the heterolytic O−O bond cleavage.

For comparison, we re-examined the sulfoxidation of **S1** via initial homolysis of ^{2}**1**.[38] The overall reaction is controlled by the first step of the homolytic cleavage of the O−O bond. The TS energy for this step is shown in Figure 1 by the blue energy bar. It is seen that the barrier is 14.6 kcal mol^{-1}. Comparison of the barriers for the homolytic and heterolytic processes clearly shows that the latter mechanism is highly favored for sulfoxidation by $Fe^{III}(H_2O_2)$.

Presumably, $Fe^{III}(H_2O_2)$ may also produce Cpd I by shunting the native cycle. In the absence of a base that may

dx.doi.org/10.1021/ct400190f | J. Chem. Theory Comput. XXXX, XXX, XXX−XXX

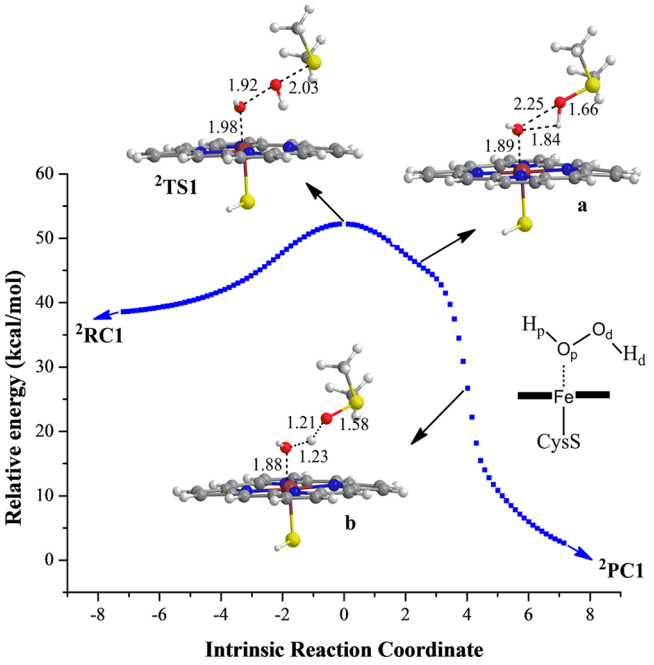

Figure 2. The calculated intrinsic reaction coordinate (IRC) from ^{2}**TS1**. **a** and **b** are two snapshot structures along the IRC. The group charge distribution in **a** is +0.81 on the DMS−OH fragment and −0.81 on the rest (see Table S1). The right-hand structure shows the atomic labels on H_2O_2.

catalyze Cpd I formation,[13] $Fe^{III}(H_2O_2)$ will form Cpd I by a homolytic mechanism.[45] Indeed, as shown before,[45,46] we find here too that the conversion of $Fe^{III}(H_2O_2)$ to Cpd I involves a homolysis/hydrogen atom transfer. Initially, the O−O bond undergoes homolysis to form $Fe^{III}OH$ and an OH radical via $^2TS_{O-O}$, which already appears in Figure 1. Subsequently, the $OH^\bullet$ radical abstracts an H atom from the $Fe^{III}OH$ complex, yielding Cpd I and water. As shown in Figure 1 (the blue bar), the computed barrier for the rate determining homolysis step via $^2TS_{O-O}$ is 14.6 kcal mol^{-1}. Therefore, ^{2}**1** will sulfoxidate **S1** by a heterolytic mechanism *much faster* than it can convert to Cpd I via the homolysis mechanism. Hence, Cpd I will be bypassed in the P450 cycle *in the presence of* ^{2}***1*** *and DMS*.

To explore the generality of the Lewis acid-catalyzed sulfoxidation by H_2O_2, we also considered the synthetic iron complexes **2** and **3**. Complex **2** is an analogue of P450 with Cl as an axial ligand,[47] and **3** is an iron-corrolazine compound.[24] As shown in Figures 3 and 4, both $Fe^{III}(H_2O_2)$ complexes sulfoxidate **S1** in a concerted asynchronous heterolytic process, with activation barriers of 11.0 kcal mol^{-1} (Figure 3) for ^{4}**2** and 8.3 kcal mol^{-1} (Figure 4) for ^{4}**3**. For both species, we also examined the sulfoxidation reaction by means of a homolytic O−O cleavage, followed by $OH^\bullet$ radical attack on the sulfur center of **S1**. The calculated activation barriers for O−O homolysis are 21.3 kcal mol^{-1} for **2** (Figure S11) and 17.5 kcal mol^{-1} for **3** (Figure S13). The second step has a very small barrier, as in the case when using **1** (Figure S6). Clearly, for **2** and **3** reacting with **S1**, the concerted heterolysis mechanism is much more favorable than the homolysis mechanism. Since the TS for homolysis is also en route to corresponding Cpd I formation, these homolysis barriers also determine the corresponding rates of Cpd I formation. As such, the sulfoxidation reaction will proceed via the concerted heterolysis mechanism in these iron compounds and bypass the respective Cpd I species. Furthermore, this mechanism is favored over sulfoxidation by the corresponding Cpd 0 species via the homolytic pathway (Figure S14). Thus, in the absence of base catalysis, the $Fe^{III}(H_2O_2)$ complexes of **2** and **3** will be the sole oxidants of **S1**.

Table 1 collects all the sulfoxidation barriers of **S1** for the lowest pathways of the three potential oxidants in P450 (all in S = 1/2). It can be seen that Cpd 0, which was commonly proposed as the "second oxidant", has the highest barriers

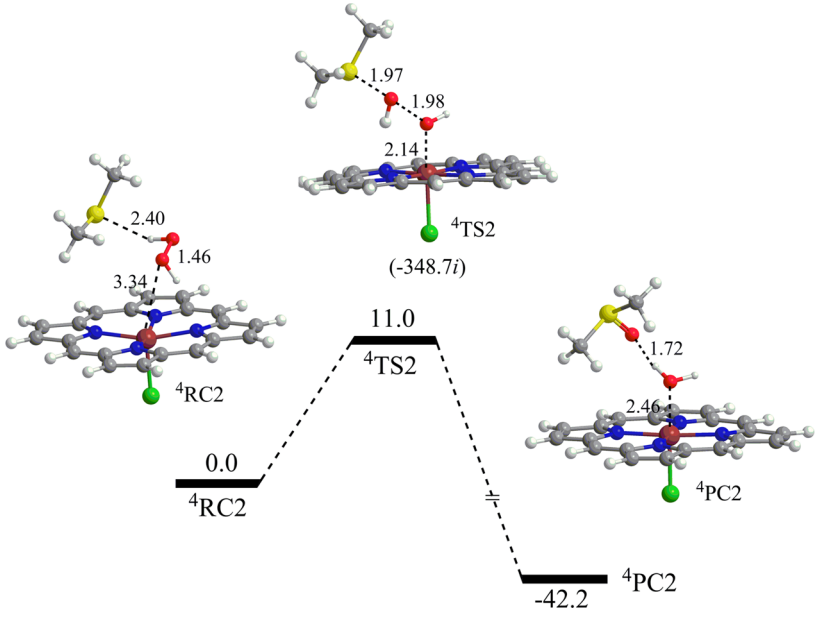

Figure 3. Calculated relative energy profile (in kcal mol^{-1}) and optimized structures (bond lengths in Å) during the concerted sulfoxidation of **S1** (DMS) by the $Fe^{III}(H_2O_2)$ complex **2**, which is an iron−porphyrin complex having a chloride axial ligand. Relative energies are given as E_2 values (UB3LYP/LACV3P++**//LACVP** with solvent correction). The value of the imaginary frequency in cm^{-1} is shown underneath the ^{4}**TS2** structure.

dx.doi.org/10.1021/ct400190f | *J. Chem. Theory Comput.* XXXX, XXX, XXX−XXX

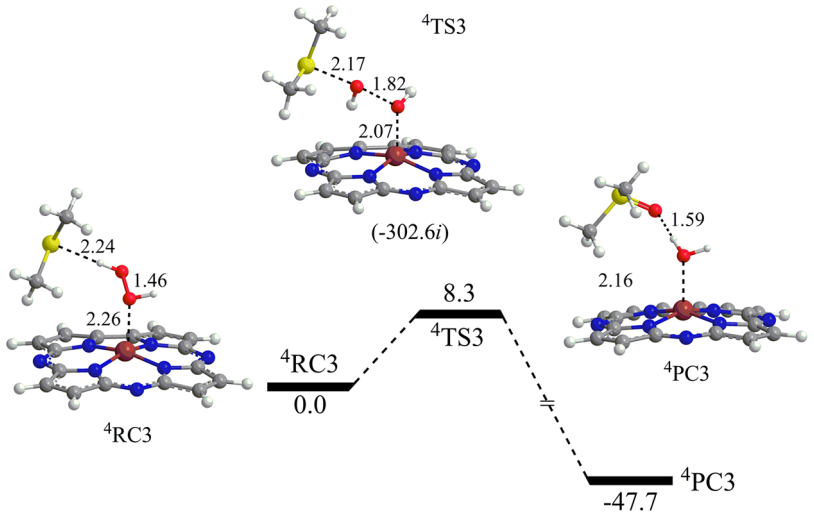

Figure 4. Calculated relative energy profile and optimized structures during the concerted sulfoxidation of **S1** (DMS) by the $Fe^{III}(H_2O_2)$ complex **3**. Relative energies (kcal mol^{-1}) are given as E_2 values (UB3LYP/LACV3P++**//LACVP** with solvent correction). The imaginary frequency in cm^{-1} is shown underneath the ^{4}**TS3** structure.

Table 1. Calculated Barriers for the Sulfoxidation Reaction of S1 (DMS) by Different Oxidants Related to the $Fe^{III}(H_2O_2)$ complex 1

oxidant		$\Delta E^{\ddagger}$ (kcal mol^{-1})[a]
Cpd I		4.7
$Fe^{III}(H_2O_2)$ (**1**)	homolysis[b]	14.6
	heterolysis[c]	5.3
Cpd 0, $Fe^{III}OOH$	homolysis[d]	23.6

[a]Barriers correspond to E_2. All the barriers are relative to the corresponding reactant clusters, ^{2}**RC**. [b]Homolysis is the stepwise homolysis/sulfoxidation mechanism. [c]Heterolysis is the concerted heterolysis mechanism studied here. [d]The barrier in a concerted pathway for Cpd 0 is >40 kcal mol^{-1} (Figure S19).

Table 2. Energy Barriers (kcal mol^{-1}) for Sulfoxidation ($\Delta E^{\ddagger}_{SO}$) and Hydroxylation ($\Delta E^{\ddagger}_{H}$) of S2 by 1 and the Corresponding Cpd I

oxidant	$\Delta E^{\ddagger}_{SO}(E_2/E_3)$[a]	$\Delta E^{\ddagger}_{H}(E_2/E_3)$[a]
Cpd I	2.4/1.8 (4.2/3.6)[b]	1.4/1.7 (3.9/4.2)[b]
$Fe^{III}(H_2O_2)$, **1**	6.7/6.9 (7.6/7.8)[b]	15.8/15.5 (15.3/15.0)[b]

[a]E_3 refers to UB3LYP/def2-TZVP//LACVP** with solvation corrections. The barriers are relative to the corresponding reactant clusters, ^{2}**RC**. [b]The values in parentheses are free energy barriers for sulfoxidation, relative to the ^{2}**RC**s (see Table S4).

among these three oxidants. *P450 Cpd 0 is a poor electrophile, and its concerted pathway has a very high barrier* (Figure S19). The sulfoxidation barrier in the stepwise homolytic mechanism of the $Fe^{III}(H_2O_2)$ complex is also quite high. By contrast, the $Fe^{III}(H_2O_2)$ barrier in the heterolytic mechanism is quite low and is comparable to that of Cpd I. Clearly, the $Fe^{III}(H_2O_2)$ complex is a potent sulfoxidation reagent via the concerted heterolysis mechanism. Cpd 0 has a high sulfoxidation barrier and cannot compete with $Fe^{III}(H_2O_2)$, while the $OH^{\bullet}$ radical and Cpd I have a higher formation barrier (via $Fe^{III}(H_2O_2)$ homolysis) compared with the sulfoxidation barrier by $Fe^{III}(H_2O_2)$. Therefore, in the presence of $Fe^{III}(H_2O_2)$, all the other oxidant species will not participate in sulfoxidation.

To further test the idea, that the $Fe^{III}(H_2O_2)$ complex might be the long sought alternative oxidant in sulfoxidation by P450,[3,5,22,23,26−31] we investigated the oxidation of *p*-CH_3S-DMA (**S2**, Scheme 2), which undergoes sulfoxidation at the SCH_3 end along with H-abstraction at the $N(CH_3)_2$ end.[22] We recall that based on the regioselectivity for **S2** oxidation by $P450_{BM3}$ and its T268A mutant, under free rotation of **S2** in the active site, it was concluded that there might be in addition to Cpd I a second oxidant which is responsible for sulfoxidation in the absence of Cpd I.[22] To elucidate this scenario, we studied the above-described two reactions using **1** vis-à-vis the corresponding reactions using Cpd I. The mechanisms are similar to the ones presented above in Figures 1−4 and are therefore relegated to the SI (Figures S15−S18), while the barrier data are shown in Table 2.

From the first two lines, it is seen that Cpd I oxidizes both sites of **S2** with the same efficiency or a slight preference for sulfoxidation (see E_3 data in the second line). By contrast, **1** is a poor H-abstractor[48,49] from the $N(CH_3)_2$ end of the molecule, whereas it is a powerful oxidant of sulfur at the SCH_3 end. This means that if the T268A mutant does not generate Cpd I but rather leads to complex **1**,[7] it will preferentially oxidize the SCH_3 end of **S2** with an efficiency that is not too far from that of Cpd I. This is especially true since the barrier for formation of Cpd I from ^{2}**1** via ^{2}**TS**$_{O-O}$ is large (the E_2 value in Figure 1 is 14.6 kcal mol^{-1}). These results provide a plausible rationale for the intriguing results of Volz et al.[22] and Cryle and De Voss.[23]

In summary, our calculations show that $Fe^{III}(H_2O_2)$ complexes of porphyrin and corrolazine based ligands (**1**−**3**, Scheme 2) are efficient oxidant species in sulfoxidation reactions, wherein sulfur acts as a nucleophile that promotes heterolytic O−O bond cleavage coupled to proton transfer. This process is catalyzed by the Fe^{III} center. As such, in the presence of a thioether, the $Fe^{III}(H_2O_2)$ complex will bypass Cpd I formation, in accordance with experimental results in model systems.[24,25] Our results further show that in the presence of a substrate with two oxidizable sites, one of which is sulfur as in **S2** (*p*-CH_3S-DMA in Scheme 2), the $Fe^{III}(H_2O_2)$ complex of cytochrome P450 can act as a second oxidant that will replace Cpd I in the T-to-A mutants of these enzymes.

dx.doi.org/10.1021/ct400190f | J. Chem. Theory Comput. XXXX, XXX, XXX−XXX

The limiting factor on the oxidative activity of Por-$Fe^{III}(H_2O_2)$ is the stability of the complex toward dissociation to $PorFe^{III}$ + H_2O_2 (Figure S21).[50] Although the lowest state for the P450 $PorFe^{III}(H_2O_2)$ complex is the sextet S = 5/2 state (Figure S20), the P450 $PorFe^{III}(H_2O_2)$ is generated from the corresponding Cpd 0,[6,7] which has an S = 1/2 ground state. So $PorFe^{III}(H_2O_2)$ will be formed initially in the S = 1/2 state, and subsequently, there will be a competition between sulfoxidation via the S = 1/2 state of $PorFe^{III}(H_2O_2)$ and spin crossover to the dissociated $PorFe^{III}$ + H_2O_2 in S = 5/2. Predicting the quantitative aspects of the competition is beyond our present capabilities. Nevertheless, since the sulfoxidation in S = 1/2 is very fast, *if the spin-inversion dissociative process is sufficiently slow*, this will allow the fast sulfoxidation to compete with H_2O_2 dissociation.[51] $PorFe^{III}(H_2O_2)$ as such has never been detected in P450 enzymes. What has been detected routinely is the liberated H_2O_2. However, since the coordinated Por-$Fe^{III}(H_2O_2)$ is a potent sulfoxidazing agent, finding uncoupling is also an indication of the presence of the second powerful oxidant $PorFe^{III}(H_2O_2)$ that liberated the H_2O_2. By itself, sulfoxidation by the $Fe^{III}(H_2O_2)$ complex is a favorable process, both kinetically and thermodynamically. This provides a driving force for the concerted oxidation of thioethers via the heterolytic mechanism, even if $Fe^{III}(H_2O_2)$ complex is less persistent than, for example, the corresponding $Fe^{III}OOH$, which is a much poorer oxidant. These findings have implications for metalloenzymes and other metal-catalyzed oxidation of sulfur and selenium compounds, when H_2O_2 is used as a terminal oxidant.[10−12,24,25,52,53]

METHODS

The mechanism was studied using B3LYP/LACVP** for geometry optimization and frequency calculations. The correlation between the stable structures and the transition states was verified by usage of intrinsic reaction coordinate (IRC) calculations. The energy was corrected by single-point calculations with LACV3P++** (E_1 values) and bulk polarity inclusion with the SMD[54] solvent model (E_2 values). For the reactions with **S2**, we also used an all electron triple-ζ basis set, def2-TZVP,[55] which after SMD correction gave energies denoted as E_3. The zero-point energies (ZPE) are included in E_1, E_2, and E_3. All calculations were performed with the Gaussian 09 package.[56] More details can be found in the Supporting Information (SI).

ASSOCIATED CONTENT

Supporting Information

Energy profiles, geometries, and optimized Cartesian coordinates of all stationary points. This material is available free of charge via the Internet at http://pubs.acs.org.

AUTHOR INFORMATION

Corresponding Author

*E-mail: sason@yfaat.ch.huji.ac.il, wwnam@ewha.ac.kr.

Notes

The authors declare no competing financial interest.

ACKNOWLEDGMENTS

Support by the Israeli Science Foundation ISF grant 53/09 (S.S.), and NRF of Korea through CRI, WCU R31-2008-000-10010-0, and GRL 2010-00353 (W.N.) is acknowledged.

REFERENCES

(1) Ortiz de Montellano, P. R. *Cytochrome P450: structure, mechanism, and biochemistry*, 3rd ed.; Kluwer Academic/Plenum Publishers: New York, 2005.
(2) van Eldik, R. Introduction: Inorganic and Bioinorganic Mechanisms. *Chem. Rev.* **2005**, *105*, 1917−2722.
(3) Denisov, I. G.; Makris, T. M.; Sligar, S. G.; Schlichting, I. Structure and Chemistry of Cytochrome P450. *Chem. Rev.* **2005**, *105*, 2253−2277.
(4) Rittle, J.; Green, M. T. Cytochrome P450 Compound I: Capture, Characterization, and C-H Bond Activation Kinetics. *Science* **2010**, *330*, 933−937.
(5) Sono, M.; Roach, M. P.; Coulter, E. D.; Dawson, J. H. Heme-Containing Oxygenases. *Chem. Rev.* **1996**, *96*, 2841−2887.
(6) Shaik, S.; Cohen, S.; Wang, Y.; Chen, H.; Kumar, D.; Thiel, W. P450 Enzymes: Their Structure, Reactivity, and Selectivity Modeled by QM/MM Calculations. *Chem. Rev.* **2010**, *110*, 949−1017.
(7) Altarsha, M.; Benighaus, T.; Kumar, D.; Thiel, W. How is the Reactivity of Cytochrome P450cam Affected by Thr252X Mutation? A QM/MM Study for X = Serine, Valine, Alanine, Glycine. *J. Am. Chem. Soc.* **2009**, *131*, 4755−4763.
(8) Lane, B. S.; Burgess, K. Metal-Catalyzed Epoxidations of Alkenes with Hydrogen Peroxide. *Chem. Rev.* **2003**, *103*, 2457−2473.
(9) Roth, J. P.; Cramer, C. J. Direct Examination of H_2O_2 Activation by a Heme Peroxidase. *J. Am. Chem. Soc.* **2008**, *130*, 7802−7803.
(10) Klebanoff, S. J. Myeloperoxidase: Friend and Foe. *J. Leukocyte Biol.* **2005**, *77*, 598−625.
(11) Davies, M. J.; Hawkins, C. L.; Pattison, D. I.; Rees, M. D. Mammalian Heme Peroxidases: From Molecular Mechanisms to Health Implications. *Antioxid. Redox Signaling* **2008**, *10*, 1199−1234.
(12) van der Veen, B. S.; de Winther, M. P. J.; Heeringa, P. Myeloperoxidase: Molecular Mechanisms of Action and Their Relevance to Human Health and Disease. *Antioxid. Redox Signaling* **2009**, *11*, 2899−2937.
(13) Hirao, H.; Li, F.; Que, L., Jr.; Morokuma, K. Theoretical Study of the Mechanism of Oxoiron(IV) Formation from H_2O_2 and a Nonheme Iron(II) Complex: O−O Cleavage Involving Proton-Coupled Electron Transfer. *Inorg. Chem.* **2011**, *50*, 6637−6648.
(14) Li, F.; England, J.; Que, L., Jr. Near-Stoichiometric Conversion of H_2O_2 to Fe^{IV}═O at a Nonheme Iron(II) Center. Insights into the O−O Bond Cleavage Step. *J. Am. Chem. Soc.* **2010**, *132*, 2134−2135.
(15) Comba, P.; Rajaraman, G.; Rohwer, H. A Density Functional Theory Study of the Reaction of the Biomimetic Iron(II) Complex of a Tetradentate Bispidine Ligand with H_2O_2. *Inorg. Chem.* **2007**, *46*, 3826−3838.
(16) Bautz, J.; Bukowski, M. R.; Kerscher, M.; Stubna, A.; Comba, P.; Lienke, A.; Münck, E.; Que, L., Jr. Formation of an Aqueous Oxoiron(IV) Complex at pH 2−6 from a Nonheme Iron(II) Complex and H_2O_2. *Angew. Chem., Int. Ed.* **2006**, *45*, 5681−5684.
(17) Nam, W. High-Valent Iron(IV)−Oxo Complexes of Heme and Non-Heme Ligands in Oxygenation Reactions. *Acc. Chem. Res.* **2007**, *40*, 522−531.
(18) Cho, J.; Jeon, S.; Wilson, S. A.; Liu, L. V.; Kang, E. A.; Braymer, J. J.; Lim, M. H.; Hedman, B.; Hodgson, K. O.; Valentine, J. S.; Solomon, E. I.; Nam, W. Structure and Reactivity of a Mononuclear Non-Haem Iron(III)−Peroxo Complex. *Nature* **2011**, *478*, 502−505.
(19) de Visser, S. P.; Rohde, J.-U.; Lee, Y.-M.; Cho, J.; Nam, W. Intrinsic Properties and Reactivities of Mononuclear Nonheme Iron−Oxygen Complexes Bearing the Tetramethylcyclam Ligand. *Coord. Chem. Rev.* **2013**, *257*, 381−393.
(20) de Visser, S. P.; Kaneti, J.; Neumann, R.; Shaik, S. Fluorinated Alcohols Enable Olefin Epoxidation by H_2O_2: Template Catalysis. *J. Org. Chem.* **2003**, *68*, 2903−2912.
(21) Berkessel, A.; Adrio, J. A. Dramatic Acceleration of Olefin Epoxidation in Fluorinated Alcohols: Activation of Hydrogen Peroxide by Multiple H-Bond Networks. *J. Am. Chem. Soc.* **2006**, *128*, 13412−13420.
(22) Volz, T. J.; Rock, D. A.; Jones, J. P. Evidence for Two Different Active Oxygen Species in Cytochrome P450 BM3 Mediated

Sulfoxidation and N-Dealkylation Reactions. *J. Am. Chem. Soc.* **2002**, *124*, 9724−9725.
(23) Cryle, M. J.; De Voss, J. J. Is the Ferric Hydroperoxy Species Responsible for Sulfur Oxidation in Cytochrome P450s? *Angew. Chem., Int. Ed.* **2006**, *45*, 8221−8223.
(24) Kerber, W. D.; Ramdhanie, B.; Goldberg, D. P. H_2O_2 Oxidations Catalyzed by an Iron(III) Corrolazine: Avoiding High-Valent Iron−Oxido Species? *Angew. Chem., Int. Ed.* **2007**, *46*, 3718−3721.
(25) Zhou, X. R.; Chen, X.; Jin, Y. Q.; Markó, I. E. Evidence of Two Key Intermediates Contributing to the Selectivity of P450-Biomimetic Oxidation of Sulfides to Sulfoxides and Sulfones. *Chem. Asian J.* **2012**, *7*, 2253−2257.
(26) Vaz, A. D. N.; McGinnity, D. F.; Coon, M. J. Epoxidation of Olefins by Cytochrome P450: Evidence From Site-Specific Mutagenesis for Hydroperoxo-Iron as an Electrophilic Oxidant. *Proc. Natl. Acad. Sci. U. S. A.* **1998**, *95*, 3555−3560.
(27) Coon, M. J.; Vaz, A. D. N.; Mcginnity, D. F.; Peng, H.-M. Multiple Activated Oxygen Species in P450 Catalysis: Contributions to Specificity in Drug Metabolism. *Drug Metab. Dispos.* **1998**, *26*, 1190−1193.
(28) Toy, P. H.; Newcomb, M.; Coon, M. J.; Vaz, A. D. N. Two Distinct Electrophilic Oxidants Effect Hydroxylation in Cytochrome P-450-Catalyzed Reactions. *J. Am. Chem. Soc.* **1998**, *120*, 9718−9719.
(29) Jin, S.; Makris, T. M.; Bryson, T. A.; Sligar, S. G.; Dawson, J. H. Epoxidation of Olefins by Hydroperoxo−Ferric Cytochrome P450. *J. Am. Chem. Soc.* **2003**, *125*, 3406−3407.
(30) Nam, W.; Lim, M. H.; Lee, H. J.; Kim, C. Evidence for the Participation of Two Distinct Reactive Intermediates in Iron(III) Porphyrin Complex-Catalyzed Epoxidation Reactions. *J. Am. Chem. Soc.* **2000**, *122*, 6641−6647.
(31) Nam, W.; Ryu, Y. O.; Song, W. J. Oxidizing intermediates in cytochrome P450 model reactions. *J. Biol. Inorg. Chem.* **2004**, *9*, 654−660.
(32) Imai, M.; Shimada, H.; Watanabe, Y.; Matsushima-Hibiya, Y.; Makino, R.; Koga, H.; Horiuchi, T.; Ishimura, Y. Uncoupling of the Cytochrome P-450cam Monooxygenase Reaction by a Single Mutation, Threonine-252 to Alanine or Valine: Possible Role of the Hydroxy Amino Acid in Oxygen Activation. *Proc. Natl. Acad. Sci. U. S. A.* **1989**, *86*, 7823−7827.
(33) Martinis, S. A.; Atkins, W. M.; Stayton, P. S.; Sligar, S. G. A Conserved Residue of Cytochrome P-450 Is Involved in Heme-Oxygen Stability and Activation. *J. Am. Chem. Soc.* **1989**, *111*, 9252−9253.
(34) Yeom, H.; Sligar, S. G.; Li, H.; Poulos, T. L.; Fulco, A. J. The Role of Thr268 in Oxygen Activation of Cytochrome $P450_{BM-3}$. *Biochemistry* **1995**, *34*, 14733−14740.
(35) Truan, G.; Peterson, J. A. Thr268 in Substrate Binding and Catalysis in $P450_{BM-3}$. *Arch. Biochem. Biophys.* **1998**, *349*, 53−64.
(36) Ogliaro, F.; de Visser, S. P.; Cohen, S.; Sharma, P. K.; Shaik, S. Searching for the Second Oxidant in the Catalytic Cycle of Cytochrome P450: A Theoretical Investigation of the Iron(III)-Hydroperoxo Species and Its Epoxidation Pathways. *J. Am. Chem. Soc.* **2002**, *124*, 2806−2817.
(37) Sharma, P. K.; de Visser, S. P.; Shaik, S. Can a Single Oxidant with Two Spin States Masquerade as Two Different Oxidants? A Study of the Sulfoxidation Mechanism by Cytochrome P450. *J. Am. Chem. Soc.* **2003**, *125*, 8698−8699.
(38) Li, C.; Zhang, L.; Zhang, C.; Hirao, H.; Wu, W.; Shaik, S. Which Oxidant Is Really Responsible for Sulfur Oxidation by Cytochrome P450? *Angew. Chem., Int. Ed.* **2007**, *46*, 8168−8170.
(39) Park, M. J.; Lee, J.; Suh, Y.; Kim, J.; Nam, W. Reactivities of Mononuclear Non-Heme Iron Intermediates Including Evidence that Iron(III)−Hydroperoxo Species Is a Sluggish Oxidant. *J. Am. Chem. Soc.* **2006**, *128*, 2630−2634.
(40) Seo, M. S.; Kamachi, T.; Kouno, T.; Murata, K.; Park, M. J.; Yoshizawa, K.; Nam, W. Experimental and Theoretical Evidence for Nonheme Iron(III) Alkylperoxo Species as Sluggish Oxidants in Oxygenation Reactions. *Angew. Chem., Int. Ed.* **2007**, *46*, 2291−2294.
(41) Han, A.-R.; Jeong, Y. J.; Kang, Y.; Lee, J. Y.; Seo, M. S.; Nam, W. Direct Evidence for an Iron(IV)-Oxo Porphyrin π-cation Radical as an Active Oxidant in Catalytic Oxygenation Reactions. *Chem. Commun.* **2008**, 1076−1078.
(42) Derat, E.; Kumar, D.; Hirao, H.; Shaik, S. Gauging the Relative Oxidative Powers of Compound I, Ferric-Hydroperoxide, and the Ferric-Hydrogen Peroxide Species of Cytochrome P450 Toward C−H Hydroxylation of a Radical Clock Substrate. *J. Am. Chem. Soc.* **2006**, *128*, 473−484.
(43) Amels, R.; Elias, H.; Wannowius, K.-J. Kinetics and Mechanism of the Oxidation of Dimethyl Sulfide by Hydroperoxides in Aqueous Medium. *J. Chem. Soc., Faraday Trans.* **1997**, *93*, 2537−2544.
(44) O−O bonds are prone to undergo S_N2 type reactions with a variety of nucleophiles. See: Strukul, G. *Catalytic Oxidations with Hydrogen Peroxide as Oxidant*; Kluwer Academic Publishers: Boston, MA, 1992; pp 53.
(45) Sicking, W.; Korth, H.-G.; Jansen, G.; de Groot, H.; Sustmann, R. Hydrogen Peroxide Decomposition by a Non-Heme Iron(III) Catalase Mimic: A DFT Study. *Chem.—Eur. J.* **2007**, *13*, 4230−4245.
(46) Cho, K.-B.; Derat, E.; Shaik, S. Compound I of Nitric Oxide Synthase: The Active Site Protonation State. *J. Am. Chem. Soc.* **2007**, *129*, 3182−3188.
(47) Le Maux, P.; Simonneaux, G. First Enantioselective Iron-Porphyrin-Catalyzed Sulfide Oxidation with Aqueous Hydrogen Peroxide. *Chem. Commun.* **2011**, *47*, 6957−6959.
(48) An oxyl character is a key factor in H-abstraction, see: Dietl, N.; Schlangen, M.; Schwarz, H. Thermal Hydrogen-Atom Transfer from Methane: The Role of Radicals and Spin States in Oxo-Cluster Chemistry. *Angew. Chem., Int. Ed.* **2012**, *51*, 5544−5555.
(49) For the importance of the oxyl, see also: Groves, J. T.; Nemo, J. E. Aliphatic Hydroxylation Catalyzed by Iron Porphyrin Complexes. *J. Am. Chem. Soc.* **1983**, *105*, 6243−6248.
(50) B3LYP tends to underestimate the binding energies for van Der Waals systems. See details in the SI (Figure S21).
(51) With a difference of two units in the *S* quantum number, the spin orbit coupling of $S = 1/2$ and $S = 5/2$ is zero. Spin orbit coupling will be provided by secondary mixing of both $S = 1/2$ and $S = 5/2$ with the $S = 3/2$ state. See: Danovich, D.; Shaik, S. Spin Orbit Coupling in the Oxidative Activation of H-H by FeO^+. Selection Rules and Reactivity Effects. *J. Am. Chem. Soc.* **1997**, *119*, 1773−1786.
(52) For implication of corrole−$Mn(H_2O_2)$ in sulfoxidation, see: Mahammed, A.; Gross, Z. Albumin-Conjugated Corrole Metal Complexes: Extremely Simple Yet Very Efficient Biomimetic Oxidation Systems. *J. Am. Chem. Soc.* **2005**, *127*, 2883−2887.
(53) Roy, G.; Mugesh, G. Anti-Thyroid Drugs and Thyroid Hormone Synthesis: Effect of Methimazole Derivatives on Peroxidase-Catalyzed Reactions. *J. Am. Chem. Soc.* **2005**, *127*, 15207−15217.
(54) Marenich, A. V.; Cramer, C. J.; Truhlar, D. G. Universal Solvation Model Based on Solute Electron Density and on a Continuum Model of the Solvent Defined by the Bulk Dielectric Constant and Atomic Surface Tensions. *J. Phys. Chem. B* **2009**, *113*, 6378−6396.
(55) Weigend, F.; Ahlrichs, R. Balanced Basis Sets of Split Valence, Triple Zeta Valence and Quadruple Zeta Valence Quality for H to Rn: Design and Assessment of Accuracy. *Phys. Chem. Chem. Phys.* **2005**, *7*, 3297−3305.
(56) Frisch, M. J.; Trucks, G. W.; Schlegel, H. B.; Scuseria, G. E.; Robb, M. A.; Cheeseman, J. R.; Scalmani, G.; Barone, V.; Mennucci, B.; Petersson, G. A.; Nakatsuji, H.; Caricato, M.; Li, X.; Hratchian, H. P.; Izmaylov, A. F.; Bloino, J.; Zheng, G.; Sonnenberg, J. L.; Hada, M.; Ehara, M.; Toyota, K.; Fukuda, R.; Hasegawa, J.; Ishida, M.; Nakajima, T.; Honda, Y.; Kitao, O.; Nakai, H.; Vreven, T.; Montgomery, J. A., Jr.; Peralta, J. E.; Ogliaro, F.; Bearpark, M.; Heyd, J. J.; Brothers, E.; Kudin, K. N.; Staroverov, V. N.; Kobayashi, R.; Normand, J.; Raghavachari, K.; Rendell, A.; Burant, J. C.; Iyengar, S. S.; Tomasi, J.; Cossi, M.; Rega, N.; Millam, N. J.; Klene, M.; Knox, J. E.; Cross, J. B.; Bakken, V.; Adamo, C.; Jaramillo, J.; Gomperts, R.; Stratmann, R. E.; Yazyev, O.; Austin, A. J.; Cammi, R.; Pomelli, C.; Ochterski, J. W.; Martin, R. L.; Morokuma, K.; Zakrzewski, V. G.; Voth, G. A.; Salvador, P.;

Dannenberg, J. J.; Dapprich, S.; Daniels, A. D.; Farkas, Ö.; Foresman, J. B.; Ortiz, J. V.; Cioslowski, J.; Fox, D. J. *Gaussian 09*, revision B. 01; Gaussian, Inc.: Wallingford, CT, 2009.